Progress In Electromagnetics Research M, Vol. 97, 133–144, 2020

A Compact Wideband Antenna Using Partial Ground Plane with Truncated Corners, L-Shaped Stubs and Inverted T-Shaped Slots

Sumeet S. Bhatia[1, *] and Narinder Sharma[2]

Abstract—The design of a wideband antenna using truncated corners partial ground plane loaded with L-shaped stubs and inverted T-shaped slots has been presented in this manuscript. The different concepts and structures related to antenna designing have been employed to attain the optimized model of antenna. L-shaped stubs and inverted T-shaped slots incised in the structure of antenna improve the impedance matching and bandwidth of the proposed antenna. A fed 50 Ω microstrip line has been applied to the proposed structure for attaining distinct performance parameters like reflection coefficient, gain, and radiation pattern. The distinct structures of proposed antenna have been juxtaposed, and it is found that the structure with L-shaped stubs and inverted T-shaped slots shows improved antenna performance parameters. The designed antenna exhibits the bandwidth of 133.04% (3.14–15.62 GHz) and 16.96% (18.56–22.0 GHz) with improved reflection coefficient and gain. The proposed antenna has also been fabricated and tested for the validation of simulated and measured results, and found in good agreement with each other. The design of proposed antenna is carved on a low cost thick substrate with compact electrical size of $0.566\lambda \times 0.452\lambda \times 0.0301\lambda\,\text{mm}^3$ at 5.45 GHz frequency and can be used for different wireless applications in the frequency range 3.14–15.62 GHz and 18.56–22.0 GHz.

1. INTRODUCTION

In the past era, antennas with wideband characteristics have appeared as the most projecting technologies for wireless communication systems. These antennas are compact in size as well as maintaining the high value of gain throughout the desired frequency range. Distinct procedures have been adopted by researchers to obtain the aforesaid antenna performance such as introduction of slots in the patch or ground plane of designed antenna, defected ground structure, introduction of parasitic element, and modified ground plane. The valuable testified works are based on the various slot and stub geometries of antennas to enhance the impedance bandwidth, for example, U-shaped stub loaded antenna with different types of etched slots [1], slots loaded E-shaped patch [2], rounded corner ground plane loaded antenna [3], radiating patch engraved with two bevels [4], and miniaturization of antenna using partial ground plane [5]. Similarly, different types of antennas are also designed by using L and T shaped slots and stubs to enhance the performance of antenna. Xu et al. [6] have investigate a T-shaped stub loaded ring resonator with slot etched on the ground plane as well as on the radiating patch for different antenna applications. Bandwidth enhancement has been achieved by Song et al. [7] on the open slot antenna by using T-shaped stub. Sung [8] introduced a square ring antenna for circular polarization application by using a T-shaped feeding structure. A T-shaped slot loaded rectangular patch antenna with defected ground plane has been designed by Yadav et al. [9] to enhance the bandwidth of the designed antenna by 77.4% in the frequency range of 5.53 GHz to 12 GHz. Sharma et

Received 25 July 2020, Accepted 23 May 2020, Scheduled 13 October 2020

* Corresponding author: Sumeet Singh Bhatia (sumeet.bhatia8@gmail.com).

[1] Electronics and Communication Engineering Department, Yadavindra College of Engineering and Technology, Guru Kashi Campus, Punjabi University, Talwandi Sabo, Bathinda, Punjab, India. [2] Department of Electrical and Electronics Engineering, Amritsar College of Engineering and Technology, Amritsar, Punjab 143001, India.

al. [10] demonstrate a compact microstrip patch antenna loaded with T-shaped slots. A T-shaped patch antenna has been designed by Verma and Srivastava [11] for bandwidth enhancement from 40.065 to 81.34% in the frequency range 1.682–3.988 GHz. A T-slot has been etched in the geometry of a disk-shaped patch antenna by Ansari and Verma [12] for different wireless applications. Likewise, an L-shaped slot antenna loaded with metamaterial has been designed for bandwidth and gain enhancement by Chen et al. [13]. A circular disk patch antenna has been designed by Ansari et al. [14] for satellite and radio telecommunication by using an L-shaped slot. Das et al. [15] have designed an open-ended inverted L-shaped slot loaded patch antenna for multiband frequency applications. Zhang and Yang [16] investigate an L-shaped open slot antenna for a UAV airborne communication system.

In this paper, an antenna with wideband characteristics has been designed and investigated. Inverted T-shaped slots and L-shaped stubs are introduced in the partial ground plane with truncated corners to achieve wider bandwidth and better impedance matching characteristics. The proposed hexagonal patch shaped antenna (proposed prototype) reports wider bandwidth, improved gain, and reflection coefficient compared to the other prototypes of designed antenna. In comparison to the existing antennas reported in the state of art literature for the validation of the results, the simulated and experimental results are also compared and found in good agreement with each other. The rest of the paper is organized as follows. Section 2 presents the design evolution of proposed antenna along with the various simulated results and variation graphs of different optimized parameters of the antenna. Section 3 demonstrates the fabricated prototype and experimental results; it also gives a comparison between the results obtained for the antennas presented in previous two sections, followed by conclusion in Section 4.

2. PROPOSED ANTENNA DESIGN STAGES

This section emphasizes design stages and the analysis of parametric study of the simulated proposed antenna. The evolution of the design procedure of different prototypes of proposed wideband antenna is delineated in Figs. 1(a) to (d), whereas the final structural model of proposed antenna prototype is shown in Fig. 1(e). Primarily, the design of antenna starts with a simple structure which consists of a compact hexagonal radiating patch associated with a 50 Ω microstrip feed line (MFL) and partial ground plane (PGP) as depicted in Fig. 1(a). The proposed structures of designed antenna are printed on a low cost FR4 glass epoxy substrate of thickness $h = 1.6$ mm with dielectric constant $\varepsilon_r = 4.4$, loss tangent $\delta_e = 0.02$, mass density 19,000 kg/m^3, and resonant frequency $f_r = 5.65$ GHz. By considering above mentioned parameters, the radius of hexagonal patch is computed as $R = 7$ mm based on following equations [17].

$$R = \frac{F}{\left\{1 + \frac{2h}{\pi F \varepsilon_r}\left[\ln\left(\frac{\pi F}{2h}\right) + 1.7726\right]\right\}^{\frac{1}{2}}} \tag{1}$$

where $F = \frac{8.791 \times 10^9}{f_r \sqrt{\varepsilon_r}}$.

The perfect impedance matching is a quite cumbersome process in the case of compact sized antenna radiators. Hence, to resolve this matter, the dimensions of the PGP are modified further to acquire a wider bandwidth and perfect impedance matching as shown in Fig. 1(b). Furthermore, the PGP is modified by making the truncated corners with side length G_2 and G_3 for lower edges similar to the upper edges of the ground plane to obtain the truncated corners partial ground plane (TCPGP) as shown in Fig. 1(c). After applying the truncation process on the PGP, the improvement in bandwidth and a reasonable impedance matching are obtained. However to achieve the desired parameters and objectives, L-shaped stubs are loaded on the TCPGP as delineated in Fig. 1(d). The main motive of introducing the L-shaped stubs in the design is to obtain the improved performance of antenna in terms of impedance matching and bandwidth. Moreover, the couple of inverted T-shaped slots are etched from the TCPGP along with the L-shaped stubs to obtain the final geometry of proposed antenna (proposed prototype) as shown in Fig. 1(e). The optimized dimensions of proposed antenna prototype are tabulated in Table 1. The dimensions of feed line, PGP, radius of radiating patch and TCPGP along with stubs and slots play a very important role to attain better impedance matching. Similarly, the inverted T-shaped slots and L-shaped stubs help in improving the antenna parameters in terms

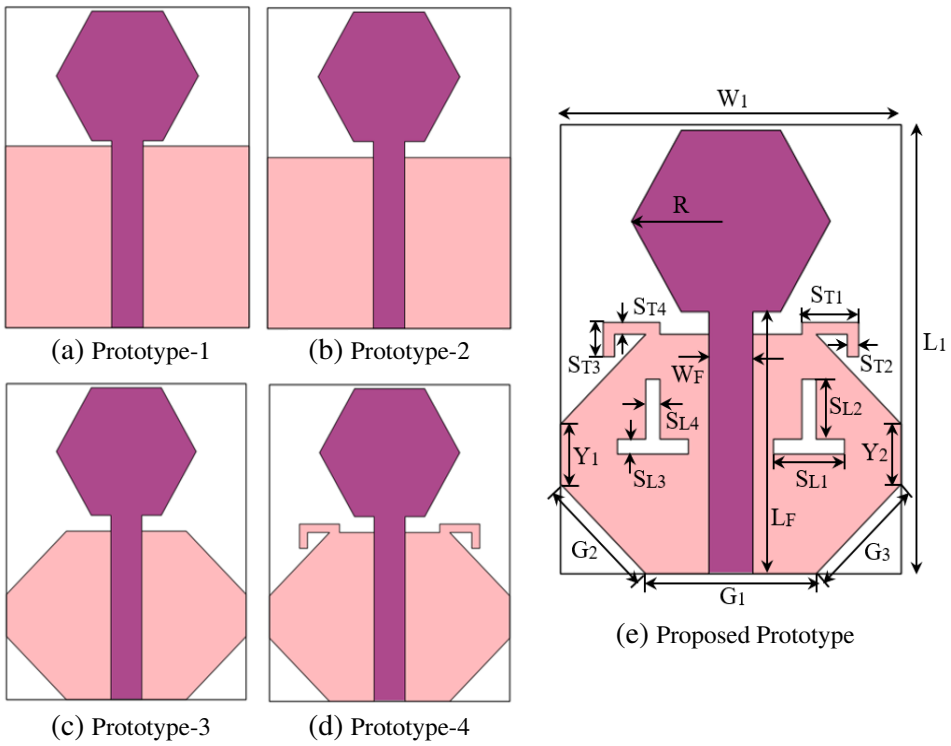

Figure 1. Design stages of the prototype of proposed antenna: (a) antenna with partial ground plane (PGP), (b) antenna with compact PGP dimensions, (c) antenna with TCPGP, (d) antenna with TCPGP and loaded with L-shaped stubs and (e) final geometry of proposed antenna with TCPGP along with L-shaped stubs and inverted T-shaped slots.

Table 1. Optimized parametric dimensions of proposed wideband antenna.

Parameters	Optimized Value (mm)	Parameters	Optimized Value (mm)	Parameters	Optimized Value (mm)
W_1	24.0	W_F	3.1	$S_{L3} = S_{L4}$	1.0
L_1	30.0	L_F	17.5	$S_{T2} = S_{T4}$	0.8
R	7.0	S_{L1}	5.0	S_{T1}	4.0
G_1	12.0	S_{L2}	4.0	S_{T3}	2.3
$G_2 = G_3$	8.48	$Y_1 = Y_2$	4.0		

of multiple resonant frequency bands with wider bandwidth and perfect impedance matching over the wide frequency range. The structures of proposed antenna have been designed, analysed, and verified by using 3D-EM (electromagnetic) solver high frequency structure simulator (HFSS) based on FEM (finite element method).

The bandwidth and impedance matching characteristics in terms of reflection coefficient of all the designed prototypes of proposed antenna are depicted in Fig. 2. It is observed from Fig. 2 that Prototype-1 exhibits the maximum bandwidth of 97.74% (3.4–9.9 GHz). The modified antenna (Prototype-2) exhibits the maximum bandwidth of 108.38% (2.9–9.75 GHz) and also shows an improved reflection coefficient in comparison to the previous design. Further, the antenna with truncated corner partial ground plane (TCPGP) exhibits the maximum bandwidth of 94.37% (7.32–20.4 GHz), and less reflection coefficient has been observed at the operational frequency ranges. After applying L-shaped stubs in the TCPGP, the antenna (Prototype-4) exhibits the maximum bandwidth of 105.22% (3.45–

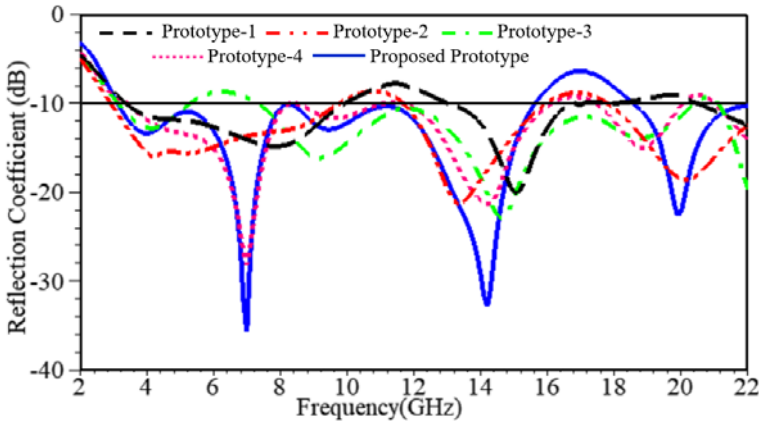

Figure 2. Reflection coefficient versus frequency plot of proposed antenna for all the designed prototypes.

11.10 GHz) and reflection coefficient of −28.10 dB at 7.0 GHz. Moreover, the inverted T-shaped stubs are etched from the antenna designed in Prototype-4 to obtain the final geometry of proposed antenna (Proposed Prototype). It is observed that the final geometry of proposed antenna exhibits an improved bandwidth of 133.04% (3.14–15.62 GHz) and improved reflection coefficients of −35.62 dB, −32.79 dB, and −22.65 dB at 7.0 GHz, 14.2 GHz, and 19.9 GHz frequency bands, respectively. It is also noticed that the improvement in reflection coefficient and bandwidth is obtained by using the modified ground plane with slots and stubs. The numerical results of all the designed prototypes along with the proposed prototype are tabulated in Table 2 for more clarity.

Furthermore, the parametric study of different dimensions of the proposed antenna such as the width of feed line (W_F) and the side length of truncated corners (G_2 and G_3) is carried out for deeper insight. The parametric analysis of aforementioned parameters is studied and investigated to achieve better impedance matching and wider bandwidth. The value of "W_F" parameter is varied

Table 2. Comparison of results for different prototypes of proposed antenna.

Antenna Design	Frequency Range (GHz)	Bandwidth (GHz)	Bandwidth Ratio	Bandwidth (%)
Prototype-1	3.4–9.9	6.5	2.91 : 1	97.74
	13.1–16.8	3.7	1.28 : 1	24.74
	20.48–22.0	1.52	1.07 : 1	7.15
Prototype-2	2.9–9.75	6.85	3.36 : 1	108.38
	11.7–15.95	4.25	1.36 : 1	30.75
	17.8–22.0	4.20	1.23 : 1	21.10
Prototype-3	3.15–5.30	2.15	1.68 : 1	50.94
	7.32–20.4	13.08	2.78 : 1	94.37
	21.12–22.0	0.8	1.04 : 1	3.71
Prototype-4	3.45–11.10	7.65	3.21 : 1	105.22
	11.75–16.10	4.35	1.37 : 1	31.25
	17.45–20.05	2.6	1.14 : 1	13.86
	21.0–22.0	1.0	1.04 : 1	4.65
Proposed Prototype	3.14–15.62	12.48	4.97 : 1	133.04
	18.56–22.0	3.44	1.18 : 1	16.96

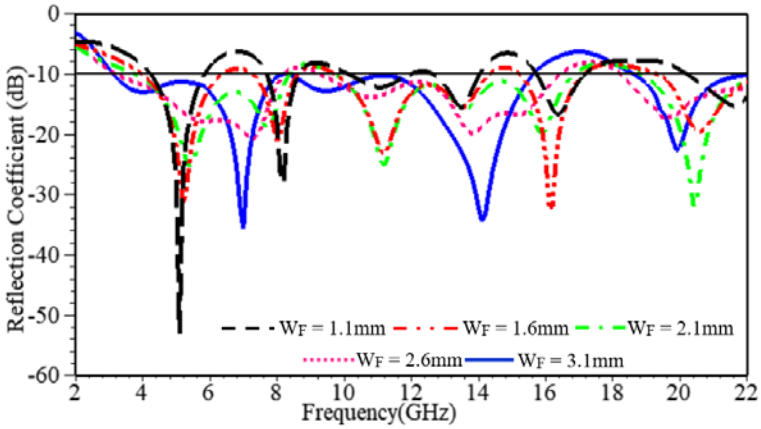

Figure 3. Effect of "W_F" parameter on the reflection coefficient of proposed antenna.

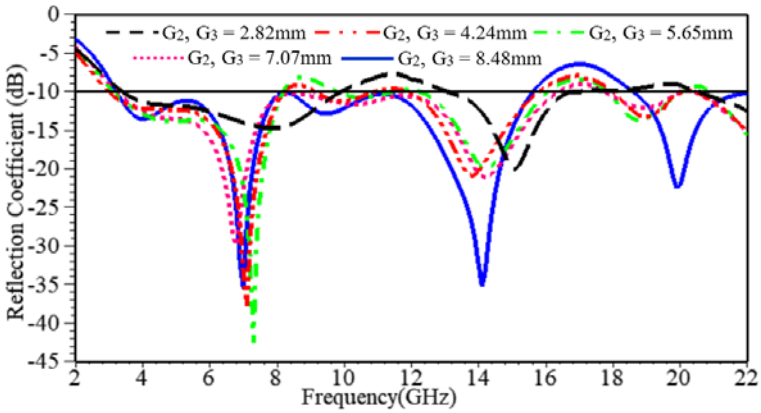

Figure 4. Effect of "G_2 and G_3" parameter on the reflection coefficient of proposed antenna.

from 1.1 mm to 3.1 mm with an increasing step size of 1.0 mm as illustrated in Fig. 3. It is analysed that at $W_F = 3.1$ mm, the antenna exhibits wider bandwidth and improved impedance characteristics in comparison to other values of W_F. Similarly, parameters G_2 and G_3 are varied to achieve better impedance characteristics as delineated in Fig. 4. It can be analysed that $G_2 = G_3 = 8.48$ mm reports better results in terms of impedance matching and bandwidth. It is also noticed that for other values of G_2 and G_3, the antenna reveals better reflection coefficient and poor bandwidth at the first resonance. Thus, optimal values (W_F, G_2, and G_3) of the proposed antenna exhibit wider bandwidth and also elucidate better reflection coefficient at higher frequency bands.

The surface current distribution of proposed wideband antenna at different resonance points are delineated in Fig. 5. It can be expounded from Fig. 5 that current is uniformly distributed on the structure of proposed antenna, and the maximum current is concentrated across feed line and ground plane which helps in the improvement of reflection coefficient of proposed antenna. The current is evenly dispersed at the L-shaped stubs which help to get the improved reflection coefficient at lower resonances. The stable current distribution near inverted T-shaped slots supports the antenna to acquire wider bandwidth within the desired frequency range. So, from the above-mentioned discussion, it is clear that effects of feedline, ground plane with slots and stubs play a very important role on the performance of proposed wideband antenna in terms of impedance bandwidth and reflection coefficient.

Group delay (ns) of the proposed wideband antenna is calculated in time domain analysis and embellished in Fig. 6. It can be perceived that the constant group delay is reported across the operational frequency range which confirms that the designed antenna can be useful for wideband operations and also work for various wireless standards. Fig. 7 illustrates the simulated real and imaginary variation

curves of input impedance, and it can be observed that the real and imaginary parts of impedance are swinging around 50 Ω to 0 Ω. Therefore, it can be claimed that resultant input impedance approximately matches the characteristic impedance of the microstrip feed line (50 Ω).

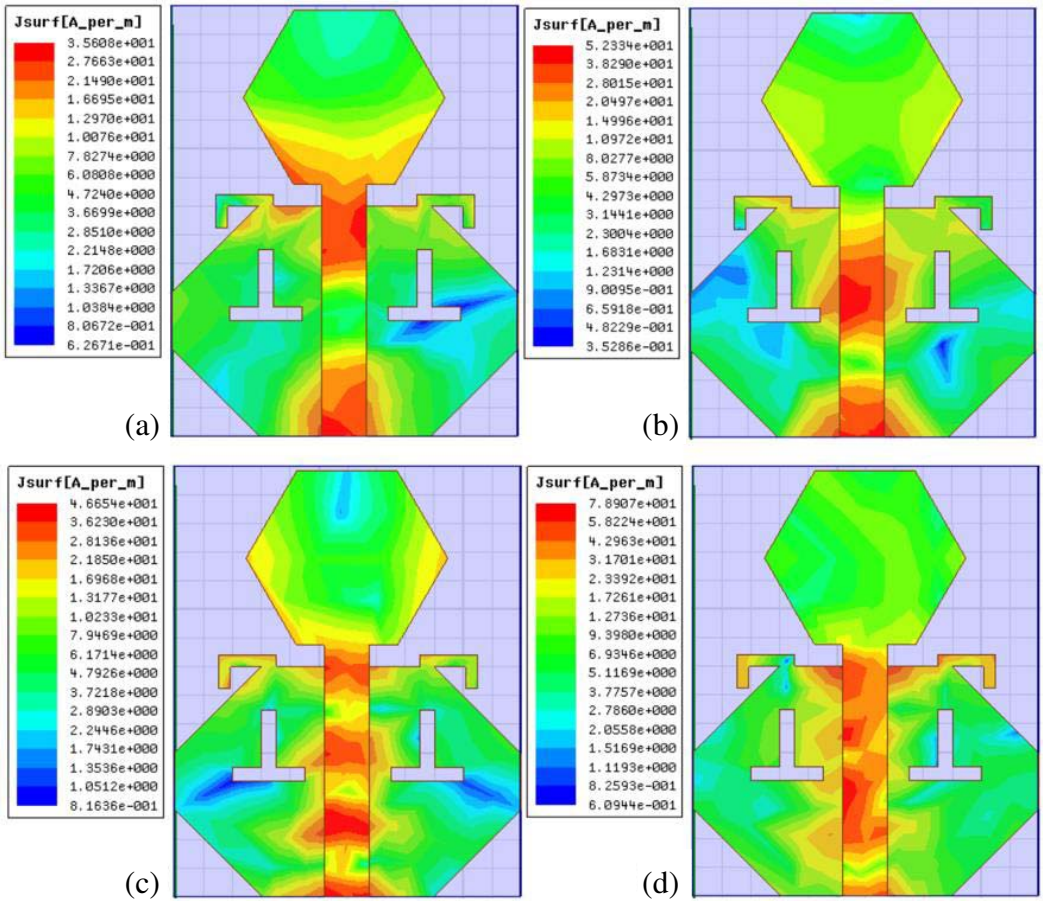

Figure 5. Simulated surface current distribution of proposed wideband antenna at different frequencies (a) 4.0 GHz, (b) 7.0 GHz, (c) 14.4 GHz and (d) 19.2 GHz.

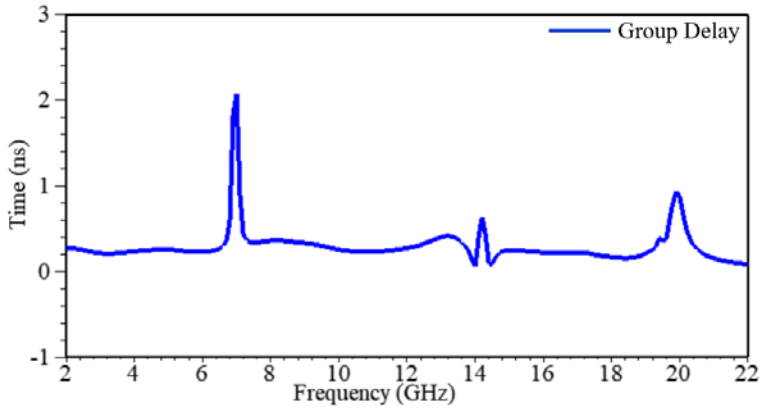

Figure 6. Group delay (nano second) versus frequency plot of proposed wideband antenna.

3. FABRICATED PROTOTYPE AND EXPERIMENTAL RESULTS

This section propounds the proposed fabricated wideband antenna along with juxtaposition of numerical and experimental results. The front and back views of the fabricated antenna are illustrated in Fig. 8, and its measurement setup is shown in Fig. 9. The proposed antenna is printed on an FR4 glass epoxy substrate of 1.6 mm thickness with overall dimensions 24 mm × 30 mm = 720 mm^2. The experimental and simulated reflection coefficients are compared and projected in Fig. 10. It can be perceived that these results are in good agreement with each other and report better impedance than the other simulated prototypes of antenna.

It is observed from Fig. 10 that simulated result (dashed black line) shows two frequency bands 7.0 GHz and 14.2 GHz in between the frequency range of 3.14–15.62 GHz with a reflection coefficient of −35.62 dB and −32.79 dB and one resonance point at 19.9 GHz in the frequency range of 18.56–22.0 GHz with reflection coefficient of −22.65 dB. Similarly, measured result (dashed red line) shows one additional frequency band at 2.9 GHz with reflection coefficient of −27.38 dB along with other two frequency bands within the frequency range 2.81–16.15 GHz, and the reflection coefficient is also less than −10 dB for the frequency range of 17.7–22.0 GHz. It is observed that the bandwidth of measured antenna is increased from 12.48 GHz to 13.34 GHz for lower frequency bands and 3.44 GHz to 4.3 GHz for higher frequency band. So, it can be anticipated that the proposed antenna acts as a good radiator for above said frequency ranges and also reports wider bandwidth, improved reflection coefficient and impedance matching. Even though the experimental and simulated results are in good agreement with each other, few of the variations are noted between these results, which may occur due to the fabrication tolerance, soldering bumps, vagueness of electrical properties of substrate, environmental conditions, etc.

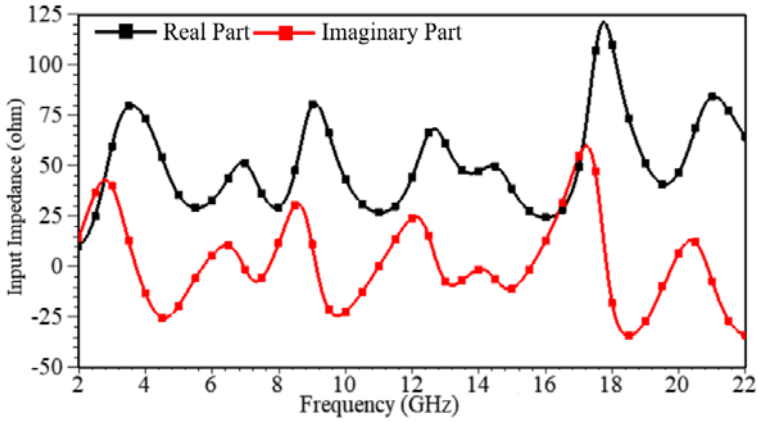

Figure 7. Input impedance curve of proposed wideband antenna.

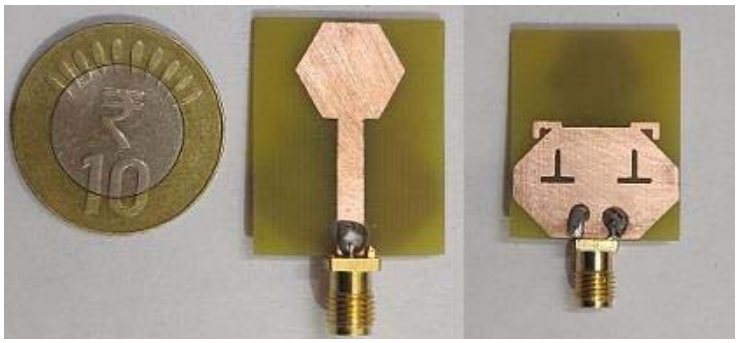

Figure 8. Front and back view of fabricated prototype of proposed wideband antenna.

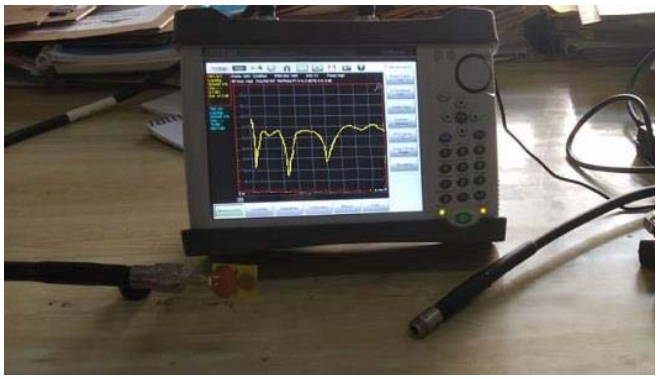

Figure 9. Measurement setup of proposed wideband antenna.

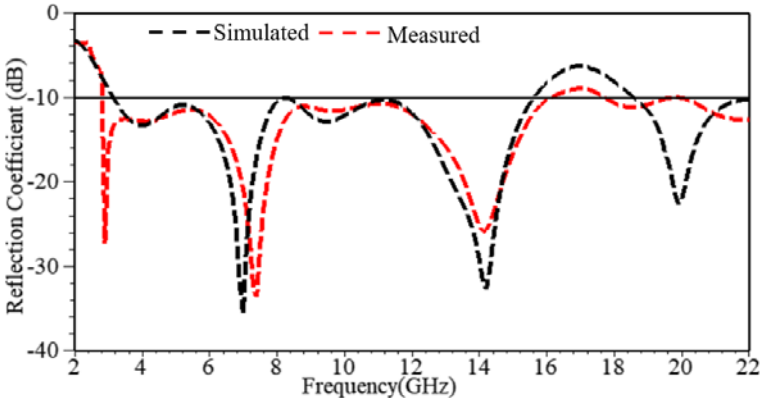

Figure 10. Reflection coefficient versus frequency curve of proposed wideband antenna.

To attain the desired results, an observant designing of fabricated structure and accurate measurement of results should be duly taken under consideration.

The radiation pattern is simulated and compared with experimental patterns to know the directional capability and behaviour of proposed wideband antenna. The comparison of simulated and measured radiation patterns in E (Y-Z) and H (X-Y) planes for different frequency bands are illustrated in Fig. 11. It can be analysed that the proposed antenna depicts a stable omnidirectional pattern in X-Y plane and dipole-like pattern in Y-Z plane at the resonant frequencies 4.0 and 7.0 GHz, whereas at higher frequency bands (14.4 and 19.2 GHz), the pattern is slightly distorted in both the planes due to the effects of asymmetric structure of ground plane (modified ground) or higher order mode generation at the higher frequencies. Gain of the proposed wideband antenna is also measured and juxtaposed with simulated gain and delineated in Fig. 12. It is predicted that simulated gain of the proposed wideband antenna is varied from 0.6 dB to 5.65 dB, whereas the measured gain is varied from 0.35 dB to 3.58 dB for the entire frequency range from 2 to 22 GHz. The variation between the values of gain is due to the fabrication tolerance and environmental conditions of the fabricated prototype of proposed antenna. The simulated and measured radiation efficiencies of proposed wideband antenna are delineated in Fig. 13. The aforementioned values of different performance parameters make the proposed antenna suitable for different wireless applications such as UWB (3.1–10.6 GHz), WiMAX (3.5–5.8 GHz), point-to-point wireless applications (5.925–8.5 GHz), C-band (4–8 GHz), ITU band (7.8–8.4 GHz), television broadcasting (7.91–8.62 GHz), FSS (11.45–11.7), X-band (8–12 GHz), broadcasting satellites (12.4–12.5 GHz), Ku-band (12–18 GHz), Ka-band (18–26 GHz), and future wireless communication applications.

The proposed antenna is juxtaposed with the existing antennas to confirm that it is optimal, and the comparison among proposed and existing antennas is delineated in Table 3. It can be anticipated

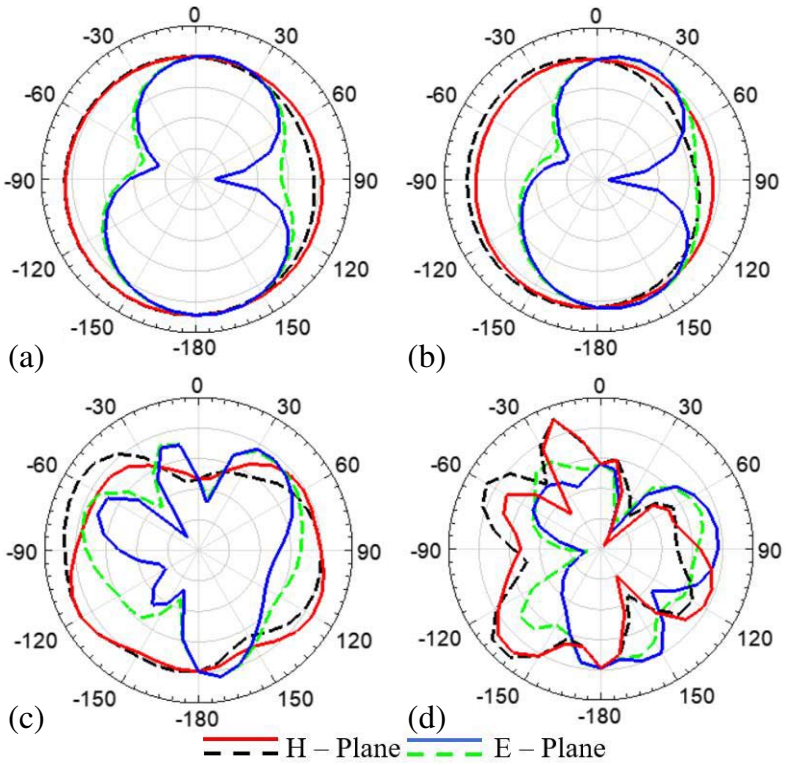

Figure 11. Radiation pattern in E (Y-Z) and H (X-Y)-plane measured (dashed) and simulated (solid) for proposed wideband antenna at (a) 4.0, (b) 7.0, (c) 14.4 and (d) 19.2 GHz frequencies.

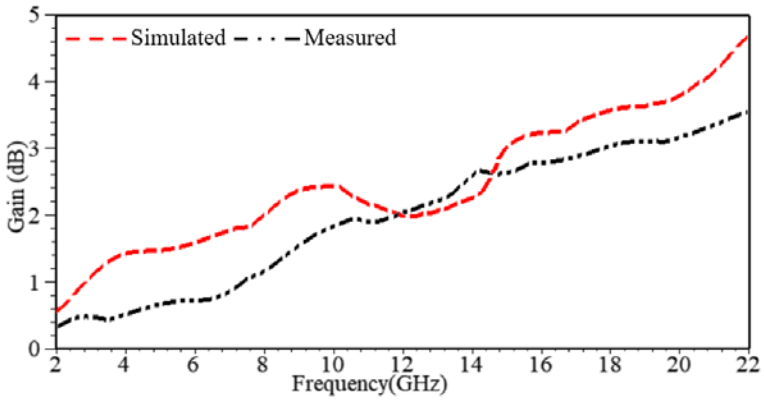

Figure 12. Gain versus frequency plot of proposed wideband antenna.

from Table 3 that proposed antenna is compact in size except the antennas reported in [26] and [27]. If th eantenna propounded in [26] is closely watched, then it can be predicted that it exhibits lesser bandwidth than the proposed antenna and does not report the gain of antenna. In the same way, the antenna projected in [27] is small in size, but other performance parameters are poor in juxtaposition to proposed antenna. On the basis of aforesaid discussion, the proposed antenna can be mentioned as a novel antenna as it reports wider bandwidth 133.04% and improved performance parameters in terms of gain, reflection coefficient, and impedance characteristics.

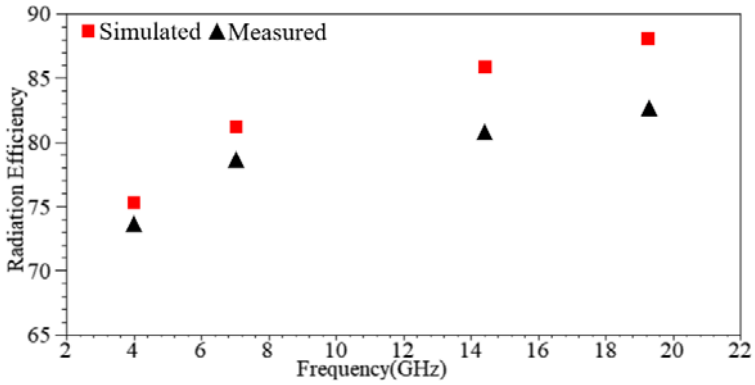

Figure 13. Radiation efficiency versus frequency plot of proposed wideband antenna.

Table 3. Comparison of proposed wideband antenna with other existing antennas of same kind.

Reference	Size of antenna (mm^3)	Space occupied (mm^2)	Maximum bandwidth (%)	Maximum gain (dB)
[18]	$37 \times 37 \times 1.6$	1369	80	5.2
[19]	$62.5 \times 12 \times 1$	750	61.1	2.37
[20]	$30 \times 30 \times 1.6$	900	94.47	4.99
[21]	$220 \times 220 \times 1.5$	48,400	148.6	4.71
[22]	$30 \times 36 \times 0.4$	1080	131.3	3.94
[23]	$45 \times 44.92 \times 1.6$	2021.4	58.50	5.1
[24]	$28 \times 28 \times 0.8$	784	129	4.2
[25]	$40 \times 38.92 \times 1.6$	1556.8	72.87	7.5
[26]	$30 \times 10 \times 1.6$	300	110	Not Specified (NS)
[27]	$20 \times 25 \times 1.6$	500	131.88	5.25
[28]	$50 \times 30 \times 2.0$	1500	100	NS
Proposed Antenna	$30 \times 24 \times 1.6$	720	133.04	5.65

4. CONCLUSION

The proposed antenna using partial ground plane with truncated corners, L-shaped stubs, and inverted T-shaped slots to improve the performance of antenna in terms of bandwidth, impedance matching, and gain has been presented in this manuscript. Various antenna structures have been designed and investigated to obtain the enhanced characteristics and optimal design of antenna. The antenna loaded with slots and stubs loaded truncated corners partial ground plane exhibits the wider bandwidth of 133.04% and 16.96% in the frequency range of (3.14–15.62 GHz) and (18.56–22.0 GHz), respectively. The proposed antenna also reports a stable radiation pattern, constant group delay, and strong concentration of current on the surface of antenna in the entire frequency range of operation. The proposed antenna is fabricated based on above theory, and results are measured. These measured results are also juxtaposed with simulated ones for the validation of prototype, and it is also found that these results are in good agreement with each other. The proposed antenna is useful for the wireless applications like UWB (3.1–10.6 GHz), WiMAX (3.5–5.8 GHz), point-to-point wireless applications (5.925–8.5 GHz), C-band (4–8 GHz), ITU band (7.8–8.4 GHz), television broadcasting (7.91–8.62 GHz), FSS (11.45–11.7), X-band (8–12 GHz), broadcasting satellites (12.4–12.5 GHz), Ku-band (12–18 GHz), Ka-band (18–26 GHz), and future wireless communication applications.

Future Scope

An improvement in any technology is a never ending process, and there is always a scope for the further improvement. So, different types of slits, slots, and stubs can be incised in the prototype for attaining the better performance in terms of gain, impedance bandwidth, reflection coefficient, etc.

REFERENCES

1. Li, P., J. Liang, and X. Chen, "Study of printed elliptical/circular slot antennas for ultrawideband applications," *IEEE Trans. Antennas Propag.*, Vol. 54, No. 6, 1670–1675, 2006.
2. Dastranj, A. and H. Abiri, "Bandwidth enhancement of printed E-shaped slot antennas fed by CPW and microstrip line," *IEEE Trans. Antennas Propag.*, Vol. 58, No. 4, 1402–1407, 2010.
3. Manohar, M., R.-S. Kshetrimayum, and A.-K. Gogoi, "A compact printed triangular monopole antenna for ultrawideband applications," *Microwave and Optical Technology Letters*, Vol. 56, No. 5, 1155–1159, 2014.
4. Jan, J.-Y. and J.-W. Su, "Bandwidth enhancement of a printed wide-slot antenna with a rotated slot," *IEEE Trans. Antennas Propag.*, Vol. 53, No. 6, 2111–2114, 2005.
5. Liang, J., C.-C. Chiau, X. Chen, and C.-G. Parini, "Printed circular disc monopole antenna for ultra-wideband applications," *Electronics Letters*, Vol. 40, No. 20, 1246, 2004.
6. Xu, K.-D., Y.-H. Zhang, J. Ronald, Y. Fan, W.-T. Joines, and Q.-H. Liu, "Design of a stub loaded ring resonator slot for antenna applications," *IEEE Trans. Antennas Propag.*, Vol. 63, No. 2, 517–524, 2015.
7. Song, K., Y.-Z. Yin, X.-B. Wu, and L. Zhang, "Bandwidth enhancement of open slot antenna with a T-shaped stub," *Microwave and Optical Technology Letters*, Vol. 52, No. 2, 390–393, 2010.
8. Sung, Y., "Stub loaded square ring antenna for circular polarization applications," *Journal of Electromagnetic Waves and Applications*, Vol. 30, No. 11, 1465–1473, 2016.
9. Yadav, N. P., M. R. Tripathy, and Y. Jeong, "T-shaped slot loaded rectangular patch antenna with enhanced bandwidth using defected ground structure," *2018 Progress In Electromagnetics Research Symposium (PIERS — Toyama)*, Japan, August 1–4, 2018.
10. Sharma, A., B.-K. Kanaujia, and S. Kumar, "Compact microstrip antenna loaded with T-shaped slots," *Int. Conf. on Microw. and Photo. (ICMAP), 2013*, 2013, doi: 10.1109/ICMAP.2013.6733495.
11. Verma, R.-K. and D.-K. Srivastava, "Bandwidth enhancement of a slot loaded T-shape patch antenna," *J. of Comput. Elect.*, Vol. 18, 205–210, 2019.
12. Ansari, J.-A. and S. Verma, "Analysis of T-slot loaded disk patch antenna for dual band operation with small frequency ratio," *Int. J. of Fut. Gener. Comm. and Netw.*, Vol. 8, No. 3, 15–30, 2015.
13. Chen, Q., H. Zhang, Y.-J. Shao, and T. Zhong, "Bandwidth and gain improvement of an L-shaped slot antenna with metamaterial loading," *IEEE Antennas and Wireless Propagation Letters*, Vol. 17, No. 8, 1411–1415, 2018.
14. Ansari, J.-A., A. Mishra, N.-P. Yadav, P. Singh, and B.-R. Vishvakarma, "Analysis of L-shaped slot loaded circular disk patch antenna for satellite and radio telecommunication," *Wireless Pers. Commun.*, Vol. 70, 927–943, 2013.
15. Das, S., P.-P. Sarkar, and S.-K. Chowdhury, "Analysis of an open-ended inverted L-shaped slot-loaded microstrip patch antenna for size reduction and multifrequency operation," *Journal of Electromagnetic Waves and Applications*, Vol. 29, No. 7, 874–890, 2015.
16. Zhang, W. and J. Yang, "Design of L-shaped open slot antenna used in UAV Airborn communication system," *Int. J. of Ant. and Propag.*, 1–13, 2018.
17. Sharma, N. and S.-S. Bhatia, "Performance enhancement of nested hexagonal ring shaped compact multiband integrated wideband fractal antennas for wireless applications," *Int. J. of RF and Microw. Comput. Aided Eng.*, Vol. 30, No. 3, 1–21, 2019.
18. Sung, Y., "Bandwidth enhancement of a microstrip line-fed printed wide-slot antenna with a parasitic centre patch," *IEEE Trans. Antennas Propag.*, Vol. 60, No. 4, 1712–1716, 2012.

19. Meng, L., W. Wang, M. Su, J. Gao, and Y. Liu, "Bandwidth extension of a printed square monopole antenna loaded with periodic parallel-plate lines," *Int. J. of Ant. and Propag.*, 1–10, 2017.
20. Sharma, N. and S.-S. Bhatia, "Double split labyrinth resonator-based CPW-fed hybrid fractal antennas for PCS/UMTS/WLAN/Wi-MAX," *Journal of Electromagnetic Waves and Applications*, Vol. 33, No. 18, 2476–2498, 2019.
21. Li, K., T. Dong, and Z. Xia, "Wideband printed wide-slot antenna with fork-shaped stub," *Electronics*, Vol. 8, No. 3, 347, 2019.
22. Yoon, C., W.-S. Kim, S.-Y. Kang, H.-C. Lee, and H.-D. Park, "Printed monopole antenna on a thin substrate for UWB applications," *Microwave and Optical Technology Letters*, Vol. 53, No. 6, 1262–1264, 2011.
23. Bhatia, S.-S. and J.-S. Sivia, "A novel design of circular monopole antenna for wireless applications," *Wireless Pers. Commun.*, Vol. 91, 1153–1161, 2016.
24. Dastranj, A. and F. Bahmanzadeh, "A compact UWB antenna design using rounded inverted L-shaped slots and beveled asymmetrical patch," *Progress In Electromagnetics Research C*, Vol. 80, 131–140, 2018.
25. Bhatia, S. S., A. Shani, and S. B. Rana, "A novel design of compact monopole antenna with defected ground plane for wideband applications," *Progress In Electromagnetics Research M*, Vol. 70, 21–31, 2018.
26. Addaci, R. and T. Fortaki, "Miniature low profile UWB antenna: New techniques for bandwidth enhancement and radiation pattern stability," *Microwave and Optical Technology Letters*, Vol. 58, No. 8, 1808–1813, 2016.
27. Tiwari, R.-N., P. Singh, and B.-K. Kanaujia, "Small-size scarecrow-shaped CPW and microstrip-line-fed UWB antennas," *J. of Comput. Elect.*, Vol. 17, 1047–1055, 2018.
28. Man, M.-Y., R. Yang, Z.-Y. Lei, Y.-J. Xie, and J. Fan, "Ultra-wideband planar inverted-F antennas with cut-etched ground plane," *Electronics Letters*, Vol. 48, No. 14, 817, 2012.